Composite Structures 386 (2026) 120296

Contents lists available at ScienceDirect

Composite Structures

journal homepage: www.elsevier.com/locate/compstruct

Mechanical and thermal properties analysis of a hedgehog spine-inspired hollow woven shape memory polymer composite

Zhengxian Liu [a,1], Lan Luo [a,1], Liwu Liu [b], Yanju Liu [b,*], Jinsong Leng [a]

[a] Center for Composite Materials and Structures, Harbin Institute of Technology (HIT), Harbin 150080, PR China
[b] Department of Astronautical Science and Mechanics, Harbin Institute of Technology (HIT), Harbin 150001, PR China

ARTICLE INFO

Keywords:
Shape memory polymer
Bio-inspired structures
3D hollow woven composites

ABSTRACT

Inspired by hedgehog spines, this study developed and investigated a new shape memory polymer composite (SMPC) that mimics the hollow-woven architecture of hedgehog spines. The hedgehog spine-inspired hollow woven SMPC exhibits high recovery force, superior energy absorption, and excellent thermal insulation performance while maintaining an ultra-low density. The material possesses a density of merely 0.12 g/cm^3, a char yield of 73.56% at 800 ℃, retaining the capacity to withstand compressive loads up to 1000 times its own weight. The maximum specific recovery force reaches 72 N/g, and even after 10 cycles of thermomechanical compression at 100 °C, the shape recovery ratio remains at 99.4%, demonstrating reliable shape memory effects and mechanical performance. Across the investigated temperatures, the material shows nearly 100% energy dissipation and excellent impact resistance. Additionally, the SMPC demonstrates outstanding thermal insulation properties. Its robust recovery under compression, torsion, and bending suggests broad potential applications in aerospace, construction, and smart textiles.

1. Introduction

Biomimetic strategies inspired by natural structures have emerged as a pivotal approach for developing novel high-performance materials [1–4]. Through millions of years of evolution, organisms have developed unique and efficient structures and mechanisms to cope with complex, changing environments. The hedgehog spines not only effectively protect hedgehogs from predators, but their lightweight, high-toughness characteristics have also attracted substantial research interest. Hedgehog spines feature a hollow, porous structure that provides resistance to local buckling with minimal weight and also offers excellent thermal insulation [5,6]. Such structural features can inherently enable efficient energy dissipation mechanisms. Energy absorption can reduce damage caused by structural vibration, making bio-inspired designs such as hedgehog spines valuable for developing advanced engineering materials [7–10]. Therefore, biological materials provide rich inspiration for the design and optimization of engineering materials.

Shape memory polymers (SMPs) are smart materials that can change shape under external stimuli and recover their original shapes via the shape memory effect [11–14]. SMPs have been widely studied for variable components and smart structures due to their shape recovery, tunable stiffness, and programmability [15–18]. Examples include deployable space structures, implantable biomedical devices, and smart textiles [19–22]. The development and application of SMPs have significantly advanced traditional materials and products [23–25]. However, SMPs still face limitations in load-carrying capacity, impact resistance, and thermal stability, which restrict their widespread use in structural applications [26,27]. To overcome these limitations and introduce additional functionalities, increasing attention has been paid to combining SMPs with reinforcements to form composites [17,28,29]. Shape memory polymer composites (SMPCs) integrate multiple constituents, leveraging complementary properties to achieve multifunctional performance [30–32]. In particular, the anisotropic behavior and constitutive modeling of woven fabric-reinforced SMPCs provide a theoretical framework for predicting their complex mechanical responses [33,34].

In recent years, hollow-woven architectures have attracted attention owing to their lightweight impact resistance and thermal insulation properties [35–37]. Li et al. [38] revealed the relationship between microstructural features and multifunctional properties of hedgehog spines using qualitative three-dimensional characterization, biomechanical analysis, and parametric simulations. Their results confirmed

* Corresponding author.
E-mail address: yj_liu@hit.edu.cn (Y. Liu).
[1] These authors contributed equally.

https://doi.org/10.1016/j.compstruct.2026.120296
Received 4 November 2025; Received in revised form 11 February 2026; Accepted 26 March 2026
Available online 28 March 2026

that hedgehog spines are biofunctionally graded, fiber-reinforced composites that can inspire lightweight, heterogeneous biomimetic designs with enhanced impact and flexural resistance. Kennedy et al. [8] investigated the effects of temperature, humidity, spine color, and their interactions on the bending strength and modulus of hedgehog spines, showing that the flexural response can be tuned by environmental conditions. Drol et al. [7] reconstructed key internal features based on the microstructure of hedgehog spines and used finite element analysis (FEA) to simulate three-point bending behavior. In contrast to these studies, this work integrates SMPs with three-dimensional hedgehog-like architectures to fabricate biomimetic SMPCs, enabling multifunctionality and high performance in a single composite structure.

This study was inspired by the microstructure of hedgehog spines, and a hedgehog spine-inspired hollow-woven SMPC was fabricated using vacuum-assisted resin transfer molding (RTM) and characterized by electron microscopy and spectroscopic analysis. The mechanical properties of the hollow-woven SMPC were evaluated via compression–recovery tests, three-point bending tests, and impact tests. The results show that the material delivers excellent driving capability and energy absorption at extremely low mass. In addition, the thermal insulation performance was assessed by examining insulation effects at different compression heights and background temperatures. The recovery behavior under compression, torsion, and bending was also evaluated, indicating potential applications in aerospace, construction, protective equipment, and smart textiles.

2. Material fabrication

Inspired by the microstructure inside a hedgehog spine (as shown in Fig. 1(a)), a three-dimensional hollow fabric was designed and manufactured. This fabric was woven by Nanjing Baipeng Textile Materials Co., Ltd., ensuring good structural integrity and uniformity, which in turn guarantees the overall performance of the material structure. The fabric was made of glass fiber. To ensure uniform and complete resin impregnation, the fabrication procedure was as follows. First, the epoxy resin (diglycidyl ether of bisphenol A, DGEBA) and curing agent (polyetheramine) were mixed at a mass ratio of 4:1. Subsequently, a 3D hollow interlayer glass fiber fabric was prepared as the reinforcement (as shown in Fig. 1(b)). The fabric was placed in a pre-prepared vacuum bag, and a vacuum pump was used to promote uniform resin infiltration throughout the architecture. After impregnation, the vacuum bag was carefully punctured, allowing the resin-impregnated fabric to recover its three-dimensional upright geometry under external pressure and elastic restoring forces. The sample was then transferred to a temperature-controlled oven for curing. The curing process is carried out according to the following temperature program: The curing schedule was as follows: 80 °C for 3 h to initiate crosslinking, 100 °C for 3 h to further develop mechanical properties, and 150 °C for 5 h to complete crosslinking. After curing, the sample was removed from the oven and cooled to ambient temperature. The cured 3D hollow interlayer woven composite was then cut to the required dimensions using mechanical cutting equipment, yielding hedgehog spine-inspired hollow-woven SMPC specimens with a density of 0.12 g/cm^3. The upper, middle, and lower microstructures of the cross-section of the hedgehog spine-inspired hollow woven SMPC are shown in Fig. 1(c). Microscopic examination of multiple specimens confirmed consistent and uniform resin impregnation within the 3D hollow-woven glass fiber fabric. Minor specimen-to-specimen variations in local fiber architecture and density were observed due to manufacturing and cutting. To ensure statistical reliability, at least five specimens were tested for each condition, and the reported mechanical, thermal, and shape memory properties represent mean values from repeated measurements.

3. Experimental

3.1. Dynamic mechanical analysis

The dynamic mechanical and shape memory properties of epoxy-based shape memory polymer under thermodynamic effects were evaluated using dynamic mechanical analysis (DMA) equipment in this study. Additionally, static mechanical tensile testing was used to evaluate the mechanical performance of SMP at different temperatures, and thermogravimetric analysis (TGA) was used to evaluate the thermal properties of SMP and SMPC. The DMA specimens of SMP had dimensions of 60 mm × 3 mm × 1.2 mm and were subjected to tensile mode with a fixed frequency of 2 Hz and sinusoidal strain applied. The

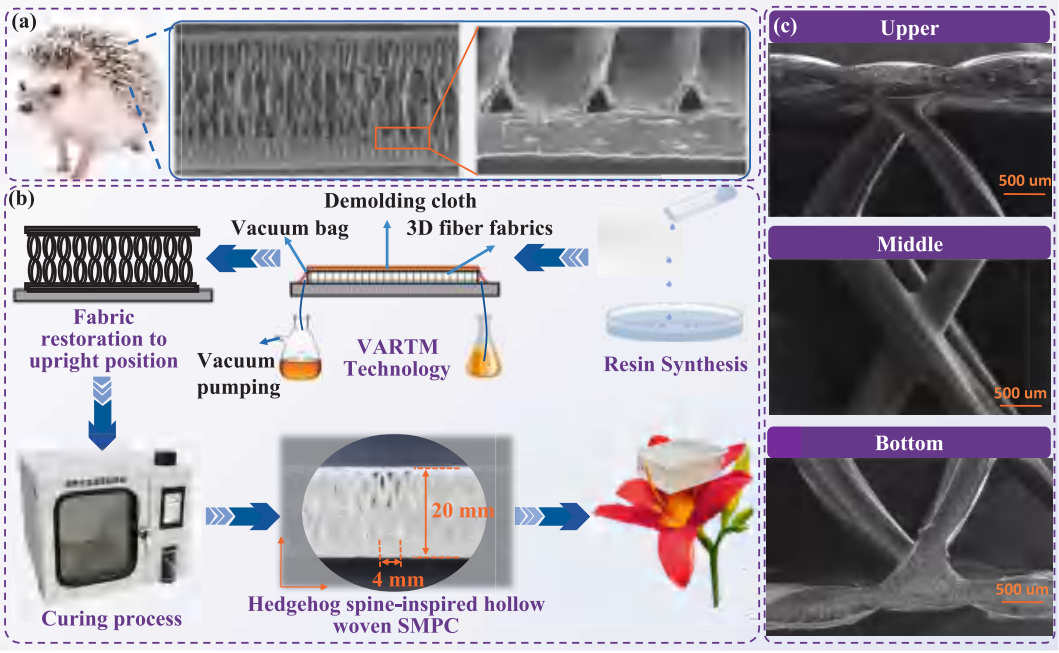

Fig. 1. The manufacturing of hedgehog spine-inspired hollow woven SMPC: (a) the microstructure inside a hedgehog spine; (b) Preparation process of hedgehog spine-inspired hollow woven SMPC; (c) Microscopic morphology of hedgehog spine-inspired hollow woven SMPC.

testing was conducted in tensile mode at a frequency of 2 Hz and a heating rate of 5 °C/min from 20 °C to 120 °C. Quantitative shape memory cycles were conducted using a DMA in controlled-force tension mode. The specimen was deformed to a maximum strain at 100 °C, cooled to 30 °C under constant load to fix the temporary shape, and subsequently unloaded. Shape recovery was triggered by reheating the sample to 100 °C. The static tensile performance testing of SMP was conducted using the ZwickRoell Z010 universal testing machine in accordance with ASTM D638 (Type IV). TGA testing was carried out using the Mettler-Toledo TGA 1 STARe model thermal gravimetric analyzer, under a high-purity nitrogen atmosphere, with a testing temperature range of 25–800 °C and a heating rate of 10 °C/min, to obtain the relationship curve between sample mass and temperature. To further study thermal stability, samples were heated at 800 °C for 5 h in a tube furnace under a high-purity nitrogen atmosphere.

3.2. Compression testing

The thermomechanical properties of SMPs exhibit significant temperature dependence. To comprehensively evaluate the dual functional characteristics of the hedgehog spine-inspired hollow woven SMPC across various application scenarios, compression tests were carried out using a ZwickRoell Z010 universal testing machine equipped with a temperature chamber. The specimen size was 60 mm × 60 mm × 20 mm. During the compression testing, a compression speed of 2 mm/min was used, and temperatures of 20 °C, 40 °C, 60 °C, 80 °C, and 100 °C were selected for testing. Samples were equilibrated at the target temperature for 10 min prior to testing. To evaluate the recovery performance at T_g, hollow woven SMPC with temporary shapes mimicking the hedgehog spines were selected for recovery testing. The force–displacement response during recovery at T_g was recorded using the force and displacement sensors. The recovery force test was conducted under constrained recovery conditions. The test was performed using a universal testing machine (Zwick Z010) equipped with a temperature chamber. The temperature was set at 100 °C, and the crosshead was raised at a constant rate of 2 mm/min to constrain the sample's recovery. The force during this process was recorded as the recovery force. Reliability was evaluated by performing 10 compression-recovery cycles (15 mm compression) at both ambient temperature and T_g.

3.3. Three-point bending testing

To comprehensively assess the bending performance and post-test morphology of the hedgehog spine-inspired hollow woven SMPC at different temperatures, three-point bending tests were conducted using a standard fixture. The specimen dimensions were 200 mm × 6 mm × 20 mm with a span of 100 mm. Bending tests were carried out at temperatures of 20 °C, 40 °C, 60 °C, 80 °C, and 100 °C with a loading speed of 2 mm/min. We recorded the displacement of the samples under gradually increasing loads and plotted the relationship curve between displacement and load. After the test was completed, we carefully observed the bending morphology of the samples, paying special attention to the microstructural changes in the damaged area. Through this evaluation, we gained a better understanding of the bending performance of the material at different temperatures and its response to external stress. Furthermore, observing the microstructural changes of the samples can also help us evaluate the material's damage tolerance, thereby better understanding its stability and durability in practical applications.

3.4. Impact performance testing

To further investigate the impact response of the hedgehog spine-inspired hollow woven SMPC under different temperatures, drop-weight impact tests were conducted to elucidate the influence of temperature on energy absorption and overall impact performance. These tests are crucial for accurately predicting the durability and safety of the material in practical applications. Firstly, the hedgehog spine-inspired hollow woven SMPC was cut into test samples of 60 mm × 60 mm × 20 mm according to standard dimensions, ensuring consistency in size and weight of each sample to guarantee reproducibility of the test results. Subsequently, we conducted tests using the standard drop hammer impact testing equipment (INSTRON 9250HV) to ensure that the energy and impact velocity during testing were controlled within predetermined ranges. The drop hammer had a mass of 6.5 kg and a hemispherical tup with a diameter of 12.7 mm. The impact energy of 10 J was achieved by adjusting the drop height. To investigate the effect of temperature on the material's impact resistance, samples were tested under different temperature conditions. Temperature control was achieved using an environmental chamber attached to the drop hammer tester. The specimen was placed inside the chamber and allowed to equilibrate at the target temperature (20 °C, 40 °C, 60 °C, 80 °C, or 100 °C) for 30 min prior to testing, as confirmed by a thermocouple embedded in a control sample. Impact was then applied to the samples, and important parameters during the impact process such as time, impact force, energy absorption, and displacement were recorded. Through these tests, we were able to comprehensively evaluate the influence of temperature variations on the material's impact resistance performance, providing important references for its performance in practical applications.

3.5. Insulation performance testing

To accurately assess the thermal insulation performance of the hedgehog spine-inspired hollow woven SMPC, the thermal insulation effect under different compression states and background temperatures were tested. A thermal imaging camera was utilized in this study to evaluate the material, aiming to simulate the thermal insulation performance at different heights in practical applications. In the experimental setup, samples were placed in a controllable temperature environment with a size of 60 mm × 60 mm × 20 mm, and compression heights were set at 0 mm, 5 mm, 10 mm, and 15 mm. To limit the compression height of the samples due to shape recovery during heating, polyimide tape was used for restraint. The temperature distribution on the top of the material at steady state was recorded, and the changes in temperature on the top side were observed over a certain period. Additionally, heating plate temperatures were set at 100 °C, 150 °C, and 200 °C to assess the temperature difference between the top and bottom surfaces of the material under different compression heights. Throughout the testing process, the environmental temperature was ensured to be stable at 20 °C, and measures were taken to avoid interference from other external heat sources on the experimental results.

3.6. Shape recovery testing

To systematically evaluate the macroscopic shape memory capability, recovery tests were conducted under compression, torsion, and bending modes via a standard thermomechanical programming cycle. The samples were initially heated to 100 ℃ and held for 10 min to ensure uniform thermal equilibrium. Subsequently, external loads were applied to induce specific deformations: vertical compression of 15 mm, torsion of 30°, and bending of 90°. These temporary shapes were fixed by cooling the specimens to ambient temperature 20 ℃ under constant constraint to freeze the molecular chain segments. After unloading, the samples were placed on a temperature chamber at 100 ℃ to trigger shape recovery. The morphological evolution was recorded in real-time using a digital camera to characterize the recovery process.

4. Results and discussion

4.1. Dynamic mechanical and thermal properties

Fig. 2(a) and (b) present the DMA test curves and shape memory cycling curves of the SMP at different temperatures. The results indicate that the T_g of the SMP is 100 ℃. As the temperature increases, the storage modulus decreases gradually, reflecting enhanced polymer chain mobility. The shape fixity ratio (R_f) and recovery ratio (R_r) were 95% and 94.7%, respectively. After three consecutive cycles, both ratios remained above 90%. Fig. 2(c) presents the tensile test curves of the SMP at different temperatures. In the glassy state, the material shows a tensile strength of 51 MPa and a fracture strain of 8.6%. As the temperature rises, the material enters the transition zone, the storage modulus rapidly decreases, and the material gradually transitions into the rubbery state. When the temperature reaches 80 ℃, the fracture strain increases to 81%, which is 8.6 times higher than at ambient temperature, while the strength at T_g decreases to 1.35 MPa, only 2.64% of the strength at ambient temperature.

Fig. 2(d) presents the TGA curves of the SMP and the hedgehog spine-inspired hollow-woven SMPC under nitrogen. Pure SMP begins to decompose at about 230 °C and leaves only 12.13% char at 800 °C, indicating almost complete thermal degradation with limited carbonaceous residue. In contrast, the SMPC shows a much higher onset decomposition temperature of −350 °C, demonstrating markedly improved thermal stability. Its char yield at 800 °C reaches 73.56%, far exceeding that of neat SMP and revealing a high fraction of thermally stable carbonaceous residue. This substantial char fraction allows the composite to retain structural integrity under extreme temperatures. Thus, the incorporation of glass fibers not only raises the decomposition onset temperature but also promotes the formation and retention of protective char, jointly enhancing the high-temperature stability and residual load-bearing capacity of the hedgehog spine-inspired hollow-woven SMPC. Fig. 2(e) and (f) depict the morphology of hedgehog spine-inspired hollow woven SMPC samples after exposure to 800 °C and the material's load-bearing demonstration. The color of the material surface changes from transparent to black, indicating the possible molecular chain breakage and carbon element accumulation to form carbides, resulting in the black color on the surface. Despite the high temperature exposure, the material maintains rigidity and strength, capable of bearing a load of 3 kg which is 1000 times its own weight.

4.2. Compression performance

Fig. 3(a) illustrates the compressive load–displacement curves of the hedgehog spine-inspired hollow woven SMPC under different temperature conditions. Across the range of 20–100 °C, all specimens exhibit a similar mechanical response: the load rises rapidly to a peak with

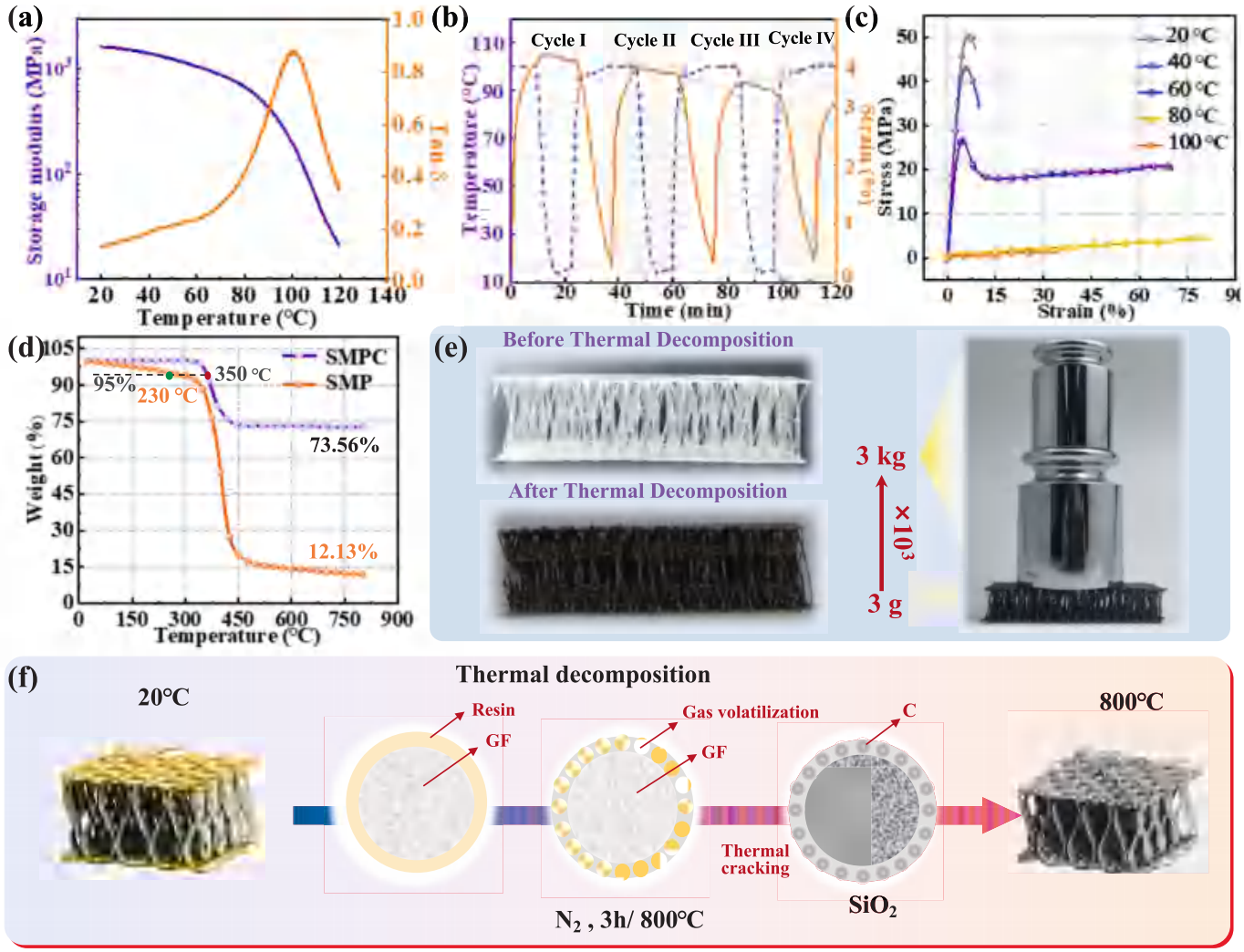

Fig. 2. Thermal analysis of shape memory materials: (a) DMA testing curve of SMP; (b) Shape memory cycle of SMP; (c) Static tensile testing curve of SMP at different temperatures; (d) TGA curves of SMP and SMPC; (e) Morphology before and after thermal decomposition; (f) Schematic diagram of thermal decomposition process of hedgehog spine-inspired hollow woven SMPC.

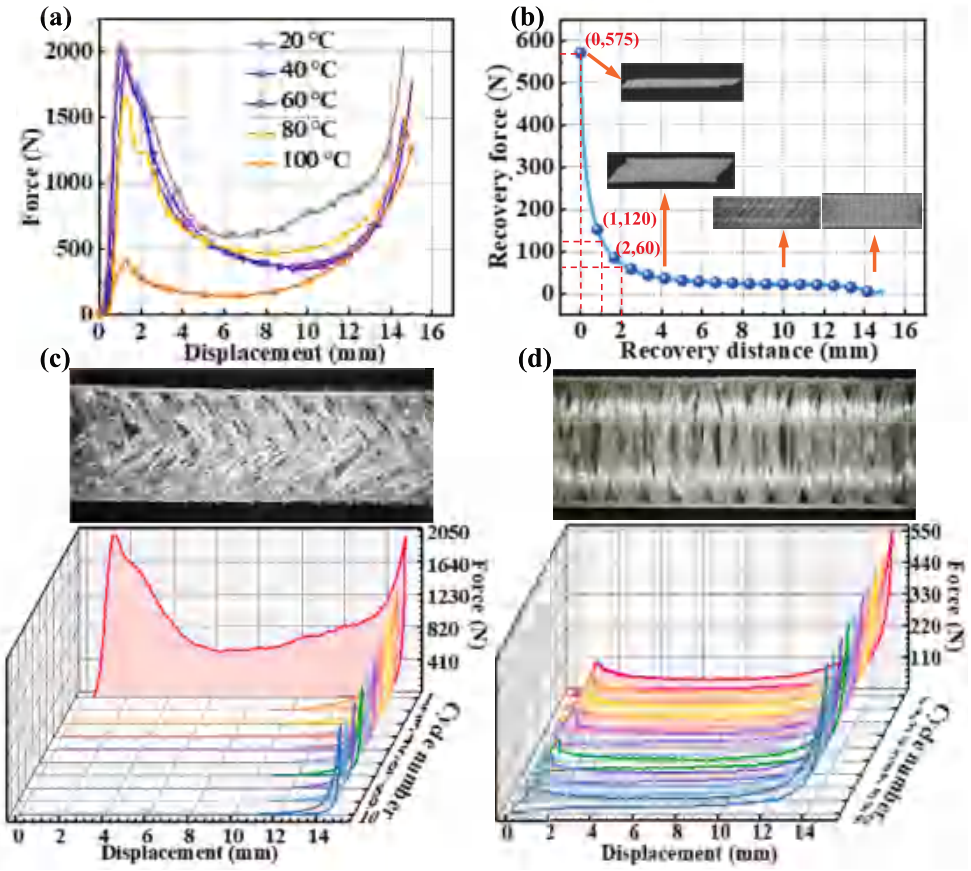

Fig. 3. Compression and recovery tests on hedgehog spine-inspired hollow woven SMPC: (a) Compression load–displacement curves at different temperatures; (b) Relationship between recovery force and recovery distance; (c) 10 cycles of compression-recovery curves at ambient temperature; (d) 10 cycles of compression-recovery curves at T_g.

increasing displacement, followed by a sudden drop. The initial linear region corresponds to elastic bending of the woven pillars, while the abrupt load decrease is associated with collective buckling of the woven fibers. As compression proceeds and the hollow architecture becomes progressively compacted, the load increases again. A closer comparison of the curves at different temperatures shows that the peak load decreases monotonically with increasing temperature. For instance, the peak load is highest at 20 °C (approximately 2.1 kN) and lowest at 100 °C (about 0.38 kN), indicating a marked reduction in load-bearing capacity at elevated temperatures due to the reduced modulus of the SMP matrix. Although matrix softening substantially lowers the peak load, the displacement at the onset of geometric buckling remains nearly unchanged, apart from minor fluctuations. The post-peak behavior also depends strongly on temperature. At lower temperatures, the load drops more steeply and the subsequent rise is more pronounced, whereas at higher temperatures, both the decline and recovery of the load are more gradual. This trend suggests that the material possesses enhanced deformability at elevated temperatures, possibly due to the decrease in shear modulus with increasing temperature.

Fig. 3(b) shows the evolution of the recovery force for a specimen compressed by 15 mm at 100 °C. The experimental results indicate that the restorative force rapidly decreases with the increase in recovery distance. When the recovery distance approaches 0 mm, the restorative force reaches the maximum value of approximately 575 N, then rapidly decreases to about 120 N as the recovery distance increases to about 1 mm, which may be related to the shape memory effect and internal stress release of the material under high compression. Subsequently, the restorative force decreases to about 60 N when the recovery distance reaches about 2 mm, and remains relatively stable within this range, until the restorative force decreases to 0 N at 15 mm. This behavior confirms that the hedgehog spine-inspired hollow-woven SMPC exhibits excellent shape recovery capability after compression near its T_g.

Fig. 3(c) and (d) compare the compression–recovery cycles at ambient temperature and near T_g. At ambient temperature, the initial compression load is high, reflecting the stiffness of the structure in its glassy state. However, the load level decreases rapidly with successive cycles, which is indicative of internal damage such as fiber fracture or microcracking of the matrix. After 10 cycles, the significant reduction in load-bearing capacity suggests irreversible damage. In contrast, near T_g, the material shows markedly different behavior. Owing to the shape memory effect and rearrangement of internal molecular chains, the load–displacement curve maintained good shape memory effect in 10 cycles, and the height recovery ratio is maintained at 99.4%. This demonstrates that at T_g the material retains its mechanical performance without pronounced degradation. Comparing the behaviors under these two conditions reveals the distinct dual-functional characteristics of the hedgehog spine-inspired hollow woven SMPC. At ambient temperature (glassy state), the material exhibits high stiffness and strength, serving as a robust load-bearing structure, although its reusability is limited by matrix brittleness. In contrast, near T_g (rubbery state), the material transitions into a highly recoverable. This contrast confirms that the material can be switched between a rigid structural mode and a resilient damping mode via temperature control, allowing it to adapt to diverse engineering requirements. The excellent height recovery ratio and energy dissipation can be attributed to the synergistic effect between the elastic 3D hollow woven fiber network and the viscoelastic SMP matrix. This continuous porous gradient structure ensures efficient stress transfer and energy distribution. While minor batch-to-batch variations

in fiber architecture may affect absolute property values, this core multifunctional synergy is inherently stable, ensuring consistent performance.

4.3. Bending performance analysis

Fig. 4(a) and (b) show the three-point bending behavior of the hedgehog spine-inspired hollow-woven SMPC at different temperatures. As temperature increases, the maximum bending load decreases, while the maximum mid-span displacement increases. This trend reflects the reduction in matrix stiffness at elevated temperatures, allowing larger deflections under lower loads. With continued loading, the load begins to decrease as pronounced bending and damage of the hollow fiber bundles occur, as illustrated in Fig. 4(c). Beyond this stage, the load rises again due to compression and densification of the fiber bundles. At 20 °C, the maximum load reached 85 N at a 6 mm displacement, while testing at the T_g temperature resulted in a maximum load decrease to 30 N. However, the material exhibited good bending performance and a high level of damage tolerance at this temperature, with no significant structural damage observed, indicating excellent flexibility and recoverability under these conditions. In contrast, at low temperatures, fracture of the central fiber bundles occurs at relatively small displacements, revealing increased brittleness and reduced bending performance. At the T_g temperature, increased mobility of the polymer chains within the material allows for better stress dispersion during loading, maintaining structural integrity and demonstrating higher flexibility and damage tolerance. This was confirmed by the observation of post-bending morphology, with no significant fiber fracture or damage observed (as shown in Fig. 4(c)). Conversely, at low temperatures, restricted mobility of the polymer chains prevents effective stress dispersion under equivalent bending forces, leading to localized stress concentration and fracture. The results suggest that the material exhibits good bending performance and damage tolerance near its T_g temperature, while showing increased brittleness under ambient temperature conditions.

4.4. Impact resistance analysis

Fig. 5(a)–(e) Show the impact load–displacement curves of the hedgehog spine-inspired hollow-woven smpc at different temperatures. as the environmental temperature increases, the maximum impact load first decreases and then increases, indicating excellent energy-absorption capability over a broad temperature range. below 80 ℃, the force–displacement curves display similar trends at all temperatures. the initial rising branch corresponds to elastic response under impact loading. between impact displacements of approximately 2–12 mm, the load decreases and fluctuates. The observed sudden load drop in the impact curve signifies the onset of structural damage, characterized by the fracture of the woven fiber reinforcement and the subsequent cracking of the polymer matrix. As the impact displacement increases, the load gradually approaches 0, indicating further curvature of the hollow fiber section, possibly accompanied by material damage, but the impactor did not fully penetrate the specimen. The energy-displacement curve reflects that the impact energy is gradually absorbed by the material, with no saturation point of energy absorption, indicating continuous energy absorption by the material. At 100 °C, the impact response differs markedly. Within a displacement range of 0–12 mm, the load remains around 200 N, after which it abruptly increases to about 4800 N and then rapidly drops to zero. The experimental results reveal a significant influence of high temperature on the material's impact performance. Fig. 5(f) plots impact displacement as a function of time at different temperatures. Below 80 °C, the rate of displacement increase gradually decreases with time at each temperature, reflecting the progressive energy absorption and stiffness of the structure. At 100 °C, the displacement–time curve is initially linear, followed by a reduction in slope, which again indicates changing deformation mechanisms and the complex interplay between the softened matrix and the hollow-woven architecture under impact.

4.5. Thermal insulation performance

Fig. 6(a) depicts the evolution of the top-surface temperature of the hedgehog spine-inspired hollow-woven SMPC at different compression heights. For all four compression levels (0, 5, 10, and 15 mm), the surface temperature increases over time, with the heating rate first accelerating and then slowing before reaching a steady state. As the compression height increases, the steady-state temperature on the top surface rises from 46 °C to 107 °C, indicating that the thermal insulation performance deteriorates as the internal air layer is reduced. Since air is

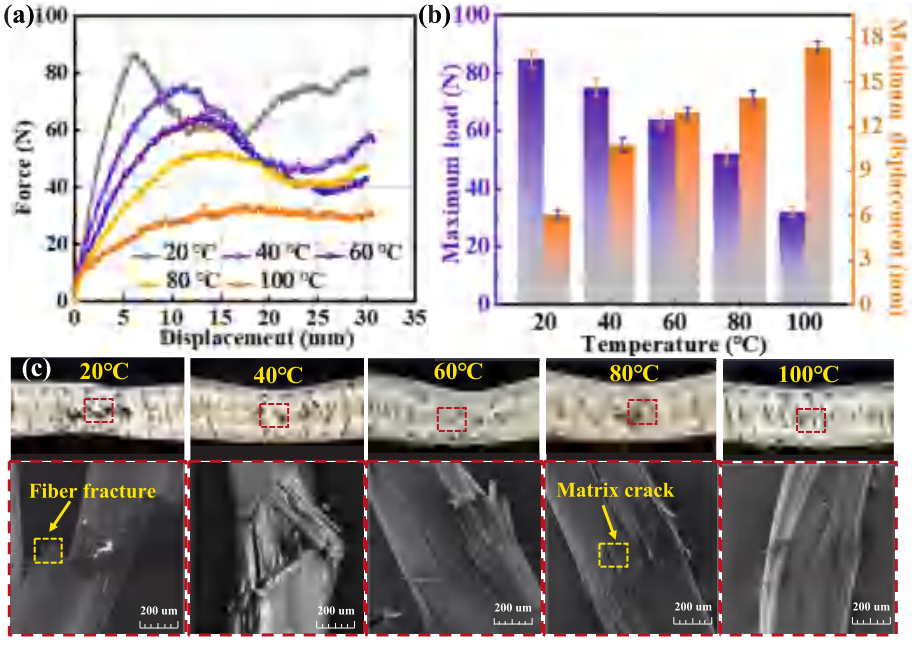

Fig. 4. Three-point bending test curves at different temperatures: (a) Load-displacement curve; (b) Maximum bending load and maximum displacement; (c) Morphology after bending test.

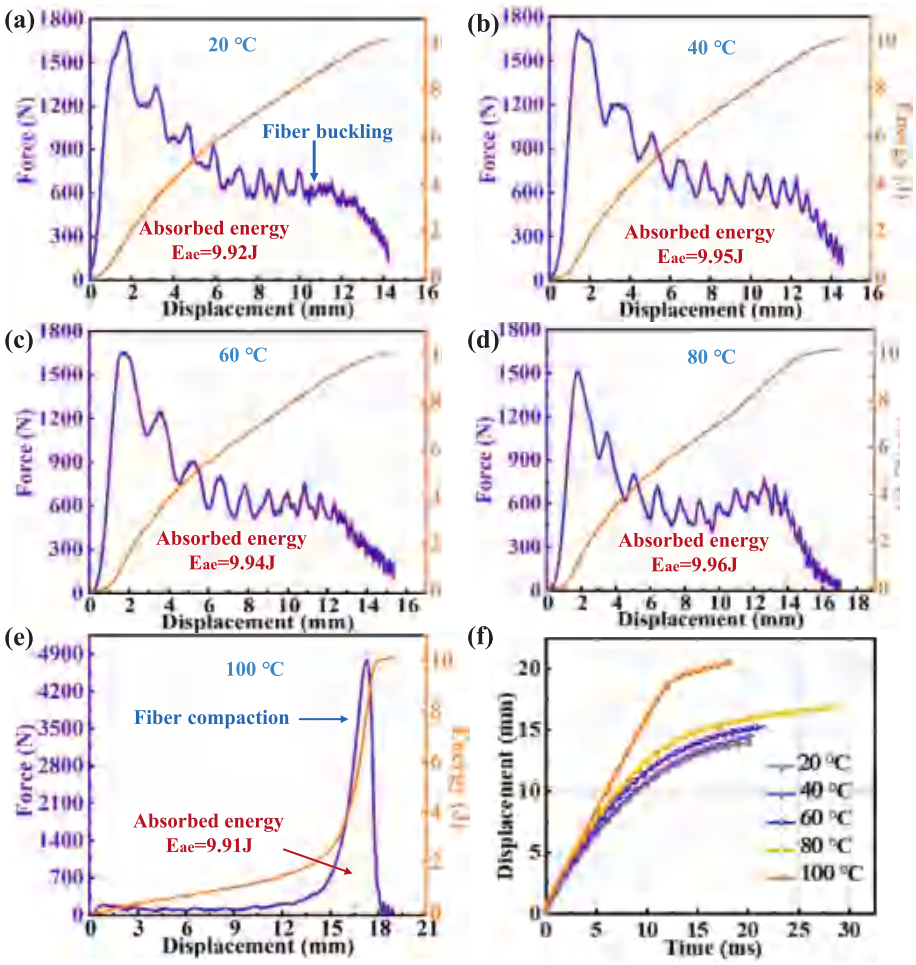

Fig. 5. (a)-(e): Relationship curves between displacement and impact load of hedgehog spine-inspired hollow woven SMPC at different temperatures; (f) The curve of impact displacement versus time at different temperatures.

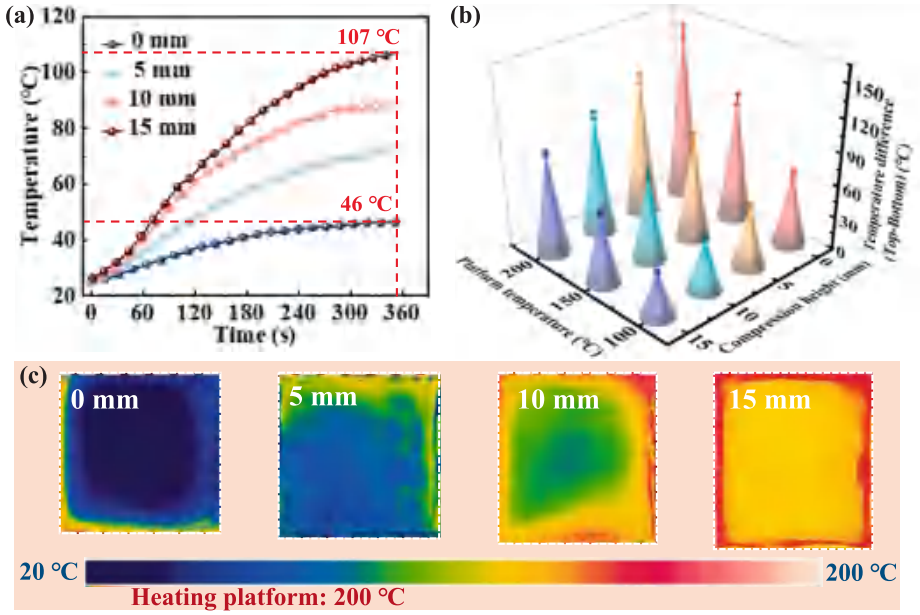

Fig. 6. Thermal insulation performance of hedgehog spine-inspired hollow woven SMPC: (a) Variation of the temperature on the upper surface with time; (b) the temperature difference between the upper and lower surfaces at different background temperatures and compression heights; (c) surface temperature distribution of the material at a background temperature of 200 ℃.

an excellent thermal insulator, decreasing its volume directly weakens the overall thermal barrier. The steady-state temperatures of 46 °C and 107 °C correspond to the uncompressed sample (h = 0 mm) and the sample compressed by 15 mm, respectively. Fig. 6(b) shows the temperature difference between the top and bottom surfaces as a function of both compression height and heating-platform temperature. The temperature difference decreases with increasing compression height, because the flattened structure conducts heat more efficiently when the hollow space is diminished. In contrast, at a fixed compression level, the temperature difference increases significantly with rising platform temperature. For example, at a compression of 10 mm, the temperature difference increases from about 68 °C at a platform temperature of 100 °C to approximately 154 °C at 200 °C. Fig. 6(c) presents the temperature distribution on the top surface of the material with a platform temperature of 200 °C. The infrared thermal imaging graph intuitively presents the temperature distribution of samples with different compression heights. The uncompressed sample (0 mm) exhibits a more uniform and lower surface temperature, whereas the highly compressed specimen (15 mm) shows higher overall temperatures and a wider distribution, with the color scale shifting toward red and yellow. These observations confirm that the hollow architecture and entrapped air volume play a crucial role in thermal insulation. Moreover, the shape memory capability of the SMPC enables active tuning of thermal insulation by reversible morphological changes. By controlling compression and recovery, the effective thickness and porosity of the structure can be adjusted, offering promising opportunities for intelligent building components or wearable devices that require adaptive thermal management.

4.6. Recovery performance

Fig. 7 illustrates the shape memory recovery behavior of the hedgehog spine-inspired hollow-woven SMPC under three macroscopic deformation modes: compression, torsion, and bending. Shape memory materials can typically return from a deformed temporary configuration to their original shape when exposed to an external stimulus such as heat, and the present SMPC demonstrates this capability consistently across all three modes. Fig. 7(a) shows the recovery process after compressive deformation. In this test, the specimen was compressed by 15 mm below Tg and subsequently cooled to fix the deformation. Upon reheating and applying a 2 kg load, the specimen recovered its original height within 100 s, corresponding to a height recovery of 15 mm and confirming outstanding shape memory performance in compression. Fig. 7(b) displays the recovery process under torsional deformation mode. The sample was twisted by 30° below T_g and cooled to lock the twisted configuration. After removing the applied torque and heating, the specimen gradually returned to its initial untwisted state, demonstrating reliable shape memory behavior under torsional loading. Fig. 7 (c) displays the bending recovery process. The specimen was bent to 90° below T_g and cooled to fix the bent shape. Upon reheating and releasing the bending moment, the sample progressively straightened and finally returned to its original configuration. The consistent recovery in all three deformation modes highlights the uniformity and integrity of the internal woven architecture and its junctions. The material can accommodate large deformations and still recover its original geometry after unloading and thermal activation. The underlying recovery mechanisms involve both fiber reorientation within the woven network and cooperative movement of polymer chain segments in the SMP matrix. This recovery behavior aligns with the anisotropic visco-hyperelastic characteristics of woven SMPCs, where the interaction between the woven architecture and the matrix plays a critical role in stress distribution and shape restoration [39].

5. Conclusions

This study systematically investigated the multifunctional performance of a bio-inspired hedgehog spine hollow woven SMPC. Fabricated via the RTM process, the composite possesses a uniform density of 0.12 g/cm^3. The material exhibited superior thermal stability; compared to pure SMP, the onset decomposition temperature increased from 230 ℃

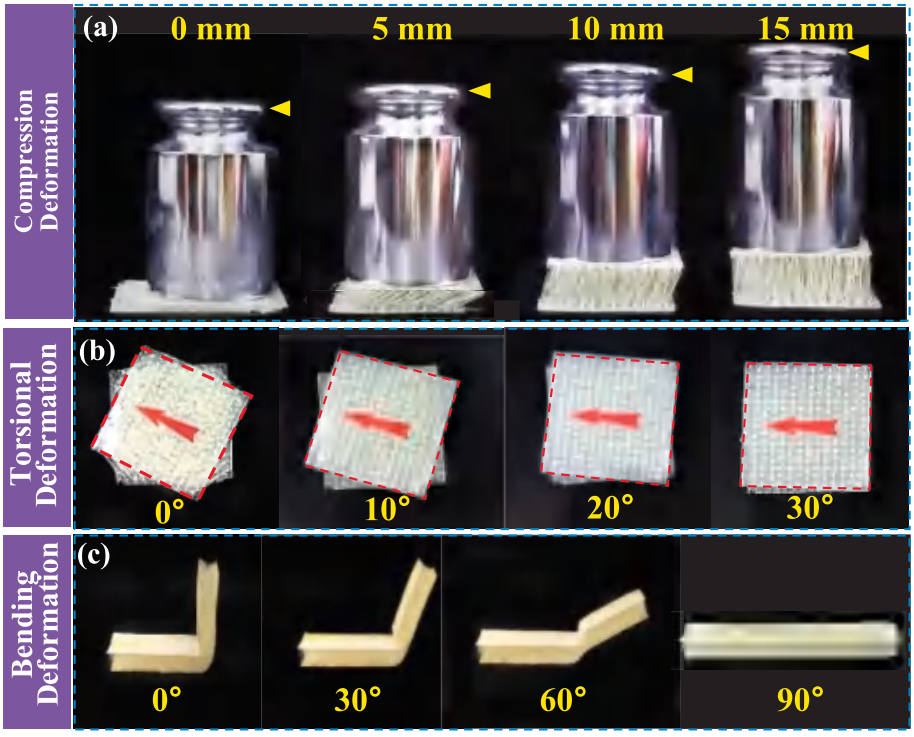

Fig. 7. Recovery process of bionic SMPC under different deformation modes: (a) compression deformation recovery process; (b) torsional deformation recovery process; (c) bending deformation recovery process.

to 350 ℃, and the char yield at 800 ℃ rose to 73.56%. Remarkably, the carbonized structure retained sufficient integrity to withstand loads 1000 times its own weight. Mechanically, the SMPC demonstrated a high specific recovery force of 72 N/g. It displayed stable shape memory effects, maintaining a shape recovery ratio of 99.4% over 10 compression cycles at 100 ℃. While the material exhibits high stiffness at ambient temperature, it transitions to a highly tough and recoverable state near T_g. Furthermore, the hollow architecture provided excellent impact resistance and thermal insulation. Under a 200 ℃ heat source, the uncompressed structure effectively mitigated heat transfer, highlighting its potential for intelligent thermal management. In conclusion, this work validates the superior multifunctional performance of the hedgehog spine-inspired SMPC, providing robust experimental evidence for the design of next-generation adaptive biomimetic structures.

CRediT authorship contribution statement

Zhengxian Liu: Writing – review & editing, Writing – original draft, Methodology, Data curation. **Lan Luo:** Validation, Methodology, Investigation, Formal analysis. **Liwu Liu:** Investigation, Formal analysis, Conceptualization. **Yanju Liu:** Supervision, Resources, Funding acquisition, Conceptualization. **Jinsong Leng:** Supervision, Resources, Conceptualization.

Declaration of competing interest

The authors declare that they have no known competing financial interests or personal relationships that could have appeared to influence the work reported in this paper.

Acknowledgements

This work was financially supported by the National Natural Science Foundation of China (Grant No. 92271206 and 12402184), the National Postdoctoral Program for Innovative Talents (Grant No. BX20230481) and the Natural Science Foundation of Heilongjiang Province (Grant No. LH2023A005).

Data availability

Data will be made available on request.

References

[1] Zhang Z, Mu Z, Wang Y, Song W, Yu H, Zhang S, et al. Lightweight structural biomaterials with excellent mechanical performance: a review. Biomimetics 2023;8:153.
[2] Wang Y, Naleway SE, Wang B. Biological and bioinspired materials: structure leading to functional and mechanical performance. Bioact Mater 2020;5:745–57.
[3] Zhang B, Han Q, Zhang J, Han Z, Niu S, Ren L. Advanced bio-inspired structural materials: local properties determine overall performance. Mater Today 2020;41:177–99.
[4] Yu H-P, Zhu Y-J. Guidelines derived from biomineralized tissues for design and construction of high-performance biomimetic materials: from weak to strong. Chem Soc Rev 2024.
[5] Yang W, McKittrick J. Separating the influence of the cortex and foam on the mechanical properties of porcupine quills. Acta Bio 2013;9:9065–74.
[6] Zhao X, Guo F, Li B, Wang G, Ye J. Multiscale simulation on the thermal response of woven composites with hollow reinforcements. Nanomaterials 2022;12:1276.
[7] Drol CJ, Kennedy EB, Hsiung B-K, Swift NB, Tan K-T. Bioinspirational understanding of flexural performance in hedgehog spines. Acta Bio 2019;94:553–64.
[8] Kennedy EB, Hsiung B-K, Swift NB, Tan K-T. Static flexural properties of hedgehog spines conditioned in coupled temperature and relative humidity environments. J Mech Behav Biomed 2017;75:413–22.
[9] Liu C, Zhao R, Yu K, Lee HP, Liao B. A quasi-zero-stiffness device capable of vibration isolation and energy harvesting using piezoelectric buckled beams. Energy 2021;233:121146.
[10] Liu C, Wang J, Zhang W, Yang X-D, Guo X, Liu T, et al. Synchronization of broadband energy harvesting and vibration mitigation via 1: 2 internal resonance. Int J Mech Sci 2025:110503.
[11] Luo L, Zhang F, Wang L, Liu Y, Leng J. Recent advances in shape memory polymers: multifunctional materials, multiscale structures, and applications. Adv Funct Mater 2023;2312036.
[12] Guo H, Puttreddy R, Salminen T, Lends A, Jaudzems K, Zeng H, et al. Halogen-bonded shape memory polymers. Nat Commun. 2022;13:7436.
[13] Duan H, Gu J, Zeng H, Khatibi AA, Sun H. A thermoviscoelastic finite deformation constitutive model based on dual relaxation mechanisms for amorphous shape memory polymers. Int J Smart Nano Mat 2023;14:243–64.
[14] Yang X, Han Z, Jia C, Wang T, Wang X, Hu F, et al. Preparation and characterization of body-temperature-responsive thermoset shape memory polyurethane for medical applications. Polymers 2023;15:3193.
[15] Luo L, Zhang F, Wang L, Liu Y, Leng J. Multidimensional cross-linked network strategies for Rapidly, Reconfigurable, refoldable shape memory polymer. Chem Eng J 2023;478:147428.
[16] Bhanushali H, Amrutkar S, Mestry S, Mhaske S. Shape memory polymer nanocomposite: a review on structure–property relationship. Polym Bull 2022;79:3437–93.
[17] Asar A, Irfan M, Khan K, Zaki W, Umer R. Self-sensing shape memory polymer composites reinforced with functional textiles. Compos Sci Technol 2022;221:109219.
[18] Xu Z, Wei D-W, Bao R-Y, Wang Y, Ke K, Yang M-B, et al. Self-sensing actuators based on a stiffness variable reversible shape memory polymer enabled by a phase change material. ACS Appl Mater Interfaces 2022;14:22521–30.
[19] Khalid MY, Arif ZU, Noroozi R, Zolfagharian A, Bodaghi M. 4D printing of shape memory polymer composites: a review on fabrication techniques, applications, and future perspectives. J Manuf Process 2022;81:759–97.
[20] Ni C, Chen D, Yin Y, Wen X, Chen X, Yang C, et al. Shape memory polymer with programmable recovery onset. Nature 2023;622:748–53.
[21] Luo L, Zhang F, Leng J. Shape memory epoxy resin and its composites: from materials to applications. Research 2022.
[22] Oladapo BI, Kayode JF, Akinyoola JO, Ikumapayi OM. Shape memory polymer review for flexible artificial intelligence materials of biomedical. Mater Chem Phys 2023;293:126930.
[23] Curtis SM, Sielenkämper M, Arivanandhan G, Dengiz D, Li Z, Jetter J, et al. TiNiHf/SiO_2/Si shape memory film composites for bi-directional micro actuation. J Smart Nano Mat 2022;13:293–314.
[24] Rokaya D, Skallevold HE, Srimaneepong V, Marya A, Shah PK, Khurshid Z, et al. Shape memory polymeric materials for biomedical applications: an update. J Compos Sci 2023;7:24.
[25] Zheng Y, Du Y, Chen L, Mao W, Pu Y, Wang S, et al. Recent advances on shape memory polymeric nanocomposites for biomedical applications and beyond. Biomater Sci 2024.
[26] Huang X, Panahi-Sarmad M, Dong K, Cui Z, Zhang K, Gonzalez OG, et al. 4D printed TPU/PLA/CNT wave structural composite with intelligent thermal-induced shape memory effect and synergistically enhanced mechanical properties. Compos Part A-Appl S 2022;158:106946.
[27] Wan T, Wang B, Han Q, Chen J, Li B, Wei S. A review of superhydrophobic shape-memory polymers: preparation, activation, and applications. Appl Mater Today 2022;29:101665.
[28] Huang X, Panahi-Sarmad M, Dong K, Li R, Chen T, Xiao X. Tracing evolutions in electro-activated shape memory polymer composites with 4D printing strategies: a systematic review. Compos Part A-Appl S 2021;147:106444.
[29] Namathoti S, Vakkalagadda MRK. Mechanical and shape recovery characterization of MWCNTs/HNTs-reinforced thermal-responsive shape-memory polymer nanocomposites. Polymers 2023;15:710.
[30] Kang D, Jeong J-M, Jeong KI, Kim SS. Sandwich type shape memory polymer composite actuators to increase the recovery moment and deformability. 20th European Conference on Composite Materials: Composites Meet Sustainability, ECCM 2022: Composite Construction Laboratory (CCLab), Ecole Polytechnique Federale de …; 2022. p. 1465-71.
[31] Namathoti S, PS RS. A review on progress in magnetic, microwave, ultrasonic responsive Shape-memory polymer composites. Mater Today: Proceedings. 2022;56:1182-91.
[32] Luo L, Zhang F, Pan W, Yao Y, Liu Y, Leng J. Shape memory polymer foam: active deformation, simulation and validation of space environment. Smart Mater Struct 2022;31:035008.
[33] Chen J, Ouyang J, Zhou X, Liao H, Du C, Zhang T, et al. Experiments and simulations on the anisotropic behavior of carbon woven fabric-reinforced shape memory polymer composites. Compos B Eng 2025:112752.
[34] Chen J, Zhou X, Du C, Wang Q, Peng X. A constitutive model for carbon fabric-reinforced shape memory polymer composites based on Eshelby's inclusion theorem. Compos Sci Technol 2025;261:111042.
[35] Lin Y, Li H, Kuang N, Chen S, Tao J. Experimental and numerical research on flexural behavior of fiber metal laminate sandwich composite structures with 3D woven hollow integrated core. J Sandw Struct Mater 2022;24:1790–807.
[36] Jeong A, Son SM, Lee S, Seong DG. Hollow glass microsphere/polydopamine/glass fiber reinforced composites with high thermal insulation performance by inhibiting conductive and radiative heat transfer. Compos Part A-Appl S 2024;179:108041.

[37] Tian X, Zhang H, Qu Z, Ai S. An efficient finite element mesh generation methodology based on μCT images of multi-layer woven composites. Compos Part A-Appl S 2024. 108255.
[38] Li Y, Zhang B, Niu S, Zhang Z, Song W, Wang Y, et al. Porous morphology and graded materials endow hedgehog spines with impact resistance and structural stability. Acta Biomater 2022;147:91–101.
[39] Su X, Wang Y, Peng X. An anisotropic visco-hyperelastic model for thermally-actuated shape memory polymer-based woven fabric-reinforced composites. Int J Plasticity 2020;129:102697.